Lab on a Chip

Miniaturisation for chemistry, physics, biology, & bioengineering

www.rsc.org/loc

Volume 9 | Number 7 | 7 April 2009 | Pages 849–1020

ISSN 1473-0197

RSC Publishing

1473-0197(2009)9:7;1-V

A new USP Class VI-compliant substrate for manufacturing disposable microfluidic devices

Jason S. Kuo, Laiying Ng, Gloria S. Yen, Robert M. Lorenz, Perry G. Schiro, J. Scott Edgar, Yongxi Zhao, David S. W. Lim, Peter B. Allen, Gavin D. M. Jeffries and Daniel T. Chiu*

Received 24th October 2008, Accepted 22nd January 2009
First published as an Advance Article on the web 10th February 2009
DOI: 10.1039/b818873d

As microfluidic systems transition from research tools to disposable clinical-diagnostic devices, new substrate materials are needed to meet both the regulatory requirement as well as the economics of disposable devices. This paper introduces a UV-curable polyurethane-methacrylate (PUMA) substrate that has been qualified for medical use and meets all of the challenges of manufacturing microfluidic devices. PUMA is optically transparent, biocompatible, and exhibits high electroosmotic mobility without surface modification. We report two production processes that are compatible with the existing methods of rapid prototyping and present characterizations of the resultant PUMA microfluidic devices.

Introduction

Microfluidic devices for clinical-diagnostic use have consistently faced a commercialization challenge: how to produce these devices economically such that they can be truly disposable while meeting the material demands of medical use. First-generation microfluidic devices, which were largely developed on silicon or glass substrates,[1–8] relied heavily on semiconductor processing tools. Because of the heavy capital investment required for processing on these substrates, silicon- or glass-based devices could not be sold inexpensively enough to be disposable.

In the late 1990s, polymer-based rapid prototyping (*e.g.* molding or embossing) led to a second generation of microfluidic devices.[9–21] Most notably, polydimethylsiloxane (PDMS) has been a very successful polymeric substrate material for rapid prototyping complex microfluidic systems.[22–25] Its mix-cast-and-bake method of replication is fast, highly consistent, and simple. As convenient as it is for rapid prototyping, PDMS is not a universal material for all microfluidic applications.[26] Although its elastomeric nature is important for pneumatic valving, this same property makes it prone to expansion when subjected to high fluidic pressure or collapse when high-aspect ratio features or low-aspect ratio channels are involved. Permanent surface modification of PDMS also remains a challenge as its surface has a high tendency to revert back to the hydrophobic state over time.[27–29]

Several new rigid substrates have been developed recently.[26,30–38] To increase the production speed, UV-curing instead of thermal curing is increasingly favored. Fiorini *et al.*[26,38] explored UV-cured thermoset polyester (TPE) as a complementary substrate material to PDMS. UV-curing of commercial optical adhesives, such as Norland 63,[39] or custom blends of polyacrylate,[40] has been proposed, but invariably due to the choice of resin or photoinitiator, only a thin layer (on the order of 100 μm) can be cured within a reasonable time. To address this issue, Fiorini *et al.*[26] used thermal curing after UV exposure to fabricate a microfluidic chip of typical thickness. However, these substrate materials have not been evaluated for medical applications and little is known about resin dissolution, reactivity, solvent residue, or crosslinking byproducts.

With increasing interest in applying microfluidic devices in clinical applications, it is important to develop substrate materials that are both economical to manufacture and can meet regulatory approval. Devoting significant time on developing the production strategy of a new substrate only to be declared non-compliant for medical use later is a significant commercialization risk. This paper introduces a polyurethane-methacrylate (PUMA) substrate – which has been certified by the supplier as United States Pharmacopeia (USP) Class VI-compliant – as a new material for the manufacturing of microfluidic devices. USP Class VI materials have been tested and proved to be biocompatible and nontoxic according to a systemic injection test, an intracutaneous test, and an implantation test.[41] Along with characterizing the physical, optical, chemical, and electrokinetic properties of the PUMA microfluidic device, we also report two replication processes of microstructures which are compatible with existing replication masters (*e.g.* SU-8-on-silicon or etched silicon), so that researchers currently utilizing other rapid-prototyping methods can benefit from using this new substrate.

Materials and methods

Optical measurement

PUMA substrates (25 mm (W) × 75 mm (L) × 2 mm (H)) were cast by pouring a UV-curable PUMA resin (140-M Medical/Optical Adhesive, Dymax Corporation) into a PDMS mold. The top surface of the resin was capped with a transparent cover, consisting of a polypropylene sheet with a peelable interfacial sheet of cellophane. The resin and mold were exposed to a high-intensity UV source (ADAC Cure Zone 2 UV Flood Light

Department of Chemistry, University of Washington, Seattle, WA, 98195-1700, USA. E-mail: chiu@chem.washington.edu; Fax: +1 206 685 8665; Tel: +1 206 543 1655

Source, fitted with a 400 W metal halide lamp, providing 80 mW cm^{-2} at 365 nm) for 1 min, then flipped over for one additional minute of exposure. The cured PUMA substrate was then released from the mold.

Thermoset polyester (TPE) pieces were prepared as described previously using Polylite 32030-10 resin (Reichhold Company, NC, USA).[10,26,38]

The optical transmission spectra were collected using a UV-VIS spectrophotometer at 1 nm resolution (Beckman Coulter, DU720). Samples of the TPE, PUMA, and PDMS were all 2 mm thick, but the glass substrate was 1 mm thick. Three spectra were collected for each material and averaged.

Autofluorescence from each material was collected using a custom-built confocal microscope based on a Nikon TE-2000 body. Laser excitation from a solid-state diode pumped 488 nm laser (Coherent Sapphire, Santa Clara, CA, USA) and a HeNe 633 nm laser was coupled into the back aperture of a 100× objective (N.A. 1.4). The laser power measured after the objective was 0.19 mW for the 488 nm laser, and 1.17 mW for the 633 nm laser; a sample area of 1 μm^2 was illuminated. Fluorescence was collected by an avalanche photo diode (SPCM-AQR-14, Perkin Elmer, Fremont, CA, USA). The fluorescence from each material was collected three times in both green wavelength range (510–565 nm) and the red wavelength region (660–710 nm).

Contact-angle measurement

PUMA slabs (25 mm (W) × 75 mm (L) × 3 mm (H)) were prepared using the same protocol as described in the previous section, except the UV-curing time was adjusted to compensate for the increased slab thickness.

To measure the contact angle, side profiles of 1 μL MilliQ water droplets on a PUMA substrate were taken with a CCD camera at ambient temperature using the static sessile drop method. Static contact angle between the water–PUMA interface and the water–air interface was measured using the Drop Analysis plug-in in ImageJ software. Contact angle on cured PDMS (75 °C for >2 h) was also taken for comparison with the literature value. A minimum of triplicate measurements were taken.

For plasma oxidation, a plasma chamber (PDC-001, Harrick Scientific Corp, Ossining, NY, USA) was used, operating at 29.6 W applied to the RF coil under a nominal O_2 pressure of 200 mTorr.

Chemical compatibility

Small PUMA discs were made by casting PUMA resin into a PDMS mold with small circular reservoirs (6 mm (D) × 3 mm (H)), covered and cured under UV. The discs were immersed in 20 different chemicals commonly encountered in microfluidic applications for 24 h at room temperature. Compatibility was determined by observing the change in the circular area of the discs at the end of the experiment. Triplicate samples were collected and the results were averaged. The top image of each disc was captured using a CCD camera under a stereoscope and the circular area was measured using ImageJ processing software.

Chemicals studied include aqueous or organic solvents, acids, bases, and dyes. To observe the penetration of dyes (Rhodamine B), fluorescence images of the PUMA discs were acquired on a Nikon AZ100 microscope (533 nm excitation).

Electroosmotic flow

The microfluidic channel for measuring EOF was a straight channel (50 μm (H) × 50 μm (W) × 3 cm (L)) with 3 mm (D) fluid reservoirs at the two ends of the channel. The electrical circuit and current-sensing elements follow the current-monitoring method described previously.[42,43] A negative-polarity programmable 2 kV DC power supply (Stanford PS350) was connected to a Pt electrode immersed in the cathode reservoir. A second electrode, immersed in the anode reservoir, was connected to a 100 kΩ resistor, in series to a Keithly 6485 picoammeter. The current read by the picoammeter was then recorded by a computer using a custom LabView program, which also controlled the output of the high-voltage power supply. Freshly sonicated sodium borate solutions were used as the buffers.

To study the effect of chip age on the electroosmotic mobility, multiple chips were prepared from three separate production runs and then simply stored in petri dishes under ambient conditions. Channels were not oxidized in plasma. The channels were stored dry (*i.e.* not filled with buffer prior to storage). Each chip was used for only one day and not re-used on subsequent days.

Results & discussion

General physical properties

The key physical and surface properties of PDMS, TPE, and PUMA are summarized in Table 1. PUMA, as based on Dymax 140-M resin, has a comparable viscosity to PDMS (Dow Corning's Sylgard 184). Significantly harder than PDMS, cured PUMA resin is more suitable for producing high-aspect ratio microstructures. Once cured, PUMA is a thermoplastic; although its service temperature as rated by the supplier is between −55 to 200 °C, we noticed some softening at >75 °C, which can be exploited for bonding. Like PDMS (but unlike TPE), PUMA has very low odor and it is not necessary to handle it under special ventilation.

Table 1 Physical properties of PDMS, TPE and PUMA

	PDMS (Sylgard 184)	TPE (Polylite 32030-01)	PUMA (Dymax 140M)
Viscosity of Resin	4600 cp	450 cp	3000 cp
After curing			
Hardness	A50	37 (Barcol)	D60
Contact Angle (water–air)	102°	61° 42° [a]	73° 53° [a] 75° [b]
Refractive Index	1.43		1.504

[a] After >5 min O_2 plasma. [b] Baked at 75 °C for 2 days following plasma treatment.

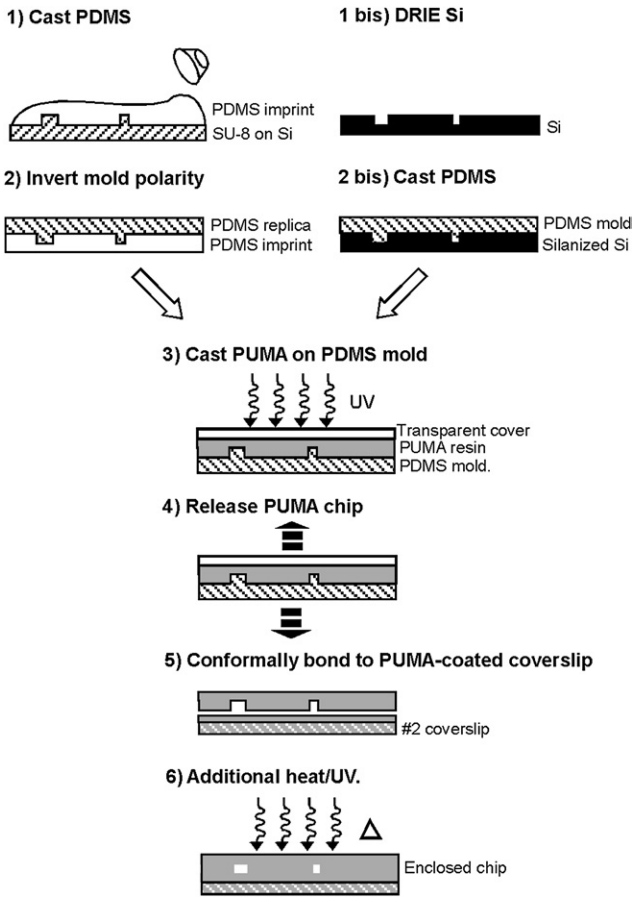

Fig. 1 Procedures for producing a PUMA chip by replicating from a SU-8 master (left branch) and from a silicon master fabricated by deep-reactive-ion-etching (DRIE) (right branch).

Feature replication

Fig. 1 shows the two procedures developed for replicating fine features onto PUMA substrates: the left branch shows the steps from a SU-8 master that was intended for producing PDMS channels, whereas the right branch shows the steps from a deep-reactive ion etched (DRIE) silicon master.

Following the left branch of Fig. 1, a SU-8 master with relief features was used to produce a PDMS imprint (*i.e.*, opposite polarity to the relief) by casting a degassed mixture of 1 : 9 (catalyst : pre-polymer) ratio of PDMS (Dow Corning Sylgard 184) and curing at 75 °C for at least 2 h. This PDMS imprint was oxidized in plasma and then silanized with (tridecafluoro-1,1,2,2-tetrahydrooctyl)trichlorosilane in a vacuum dessicator; this process prevented freshly cured PDMS from adhering to the already formed PDMS imprint. A PDMS replica (*i.e.*, same polarity as the SU-8 master) was produced by pouring additional PDMS on top of the silanized imprint, curing at 75 °C for at least 2 h, and separating carefully from the imprint. The PDMS replica (of the SU-8 master) was then used as a mold for PUMA resin; this PDMS mold is re-usable. PDMS-on-PDMS replication was needed because PUMA did not release well from SU-8. If the SU-8 master had the correct polarity, then only one PDMS replication would be sufficient. We describe this procedure so that existing SU-8 masters used for PDMS replication can be employed to make a PUMA device.

After the correct PDMS mold was obtained, PUMA resin was dispensed to 3 mm thickness onto the PDMS mold, then covered to prevent oxygen inhibition of the crosslinking reaction. To form fluidic reservoirs or holes for external connection, PTFE posts (3 mm (D) × 3 mm (H)) were embedded in the PUMA resin before curing. The entire assembly was placed in the UV source to cure. Once released from the mold, PUMA substrate was conformally bonded to another PUMA-coated (cured) glass by using gentle mechanical pressure. This conformal bond was converted to permanent bond by placing the PUMA chip under the UV flood source for an additional 10 min.

For replicating high-aspect ratio features, the mold for PUMA casting was a PDMS imprint casted on a DRIE-Si master, as described in the right branch of Fig. 1. This approach eliminates the need to produce high-aspect ratio relief features in PDMS, which are prone to leaning or buckling. Moreover, two inter-digitated pieces of PDMS, as described in the second step of the left branch in Fig. 1, are highly prone to tear during separation as the aspect ratio of the microstructure increases.

Replication fidelity

Fig. 2A shows the SEM image of a silanized PDMS imprint and Fig. 2B shows the corresponding PUMA replica (same polarity as the imprint). This PUMA replica was produced using the two-step PDMS transfer method described according to the left branch of Fig. 1. The replication fidelity was excellent, down to ~2 μm as shown in the inset of Fig. 2B. We note that the SEM image of PDMS imprint exhibited significant surface cracking; these cracks were long enough to be visible to naked eyes but they appeared to be very fine and superficial. This surface cracking behavior in the SEM images of PDMS is consistent with literature reports of prolonged plasma bombardment, likely during oxygen plasma treatment or sputtering of Au/Pd thin coating for SEM sample preparation.[44]

Fig. 3 shows more SEM images of microstructures replicated into PUMA. Fig. 3A shows a PUMA replica of a 2 μm tall microchannel constriction that is 4 μm wide at the neck. As can be seen in the SEM image, the details of the channel tapering were well preserved. Fig. 3B is a two-layer structure: the two orthogonal channels were of different height; the horizontal

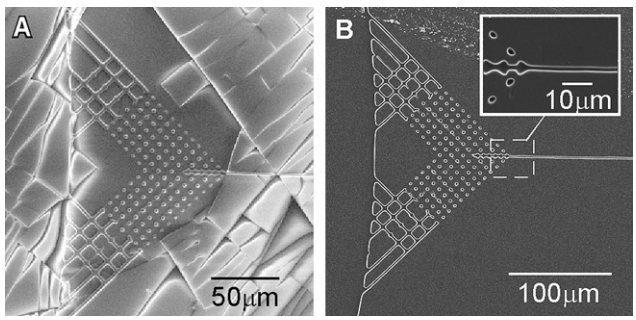

Fig. 2 SEM images of (**A**) a silanized PDMS imprint and (**B**) the corresponding PUMA replica. **Inset**: Fine details of the design at a higher magnification.

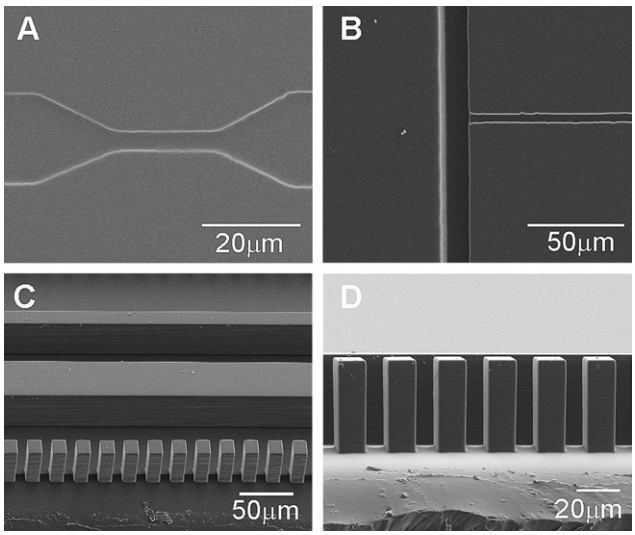

Fig. 3 SEM images of various PUMA replica. (**A**) A 2 μm (H) × 4 μm (W) constriction. (**B**) A two-layer channel structure (horizontal channel: 3 μm (W) × 3 μm (H); vertical channel: 10 μm (W) × 10 μm (H)). (**C**) A test pattern consisting of solid walls of different widths and regularly spaced columns. (**D**) Side view of the high-aspect ratio columns shown in (C).

channel was 3 μm (W) × 3 μm (H), whereas the vertical channel was 10 μm (W) × 10 μm (H).

The two-layer structure did not pose any problems for the mold-releasing step.

Fig. 3C shows the SEM image of a test pattern consisting of alternating solid walls of various width and spacing replicated in PUMA. Unlike the replicas shown in Fig. 3A and 3B, the replica in Fig. 3C was obtained by following the right branch of the procedure outlined in Fig. 1; in other words, the replication process originated from a DRIE-etched Si master. The height of the microstructures was ~40 μm. Fig. 3D is a profile-view of the columns in the lower half of Fig. 3C: these densely-spaced columns had sharp, crisp sidewalls with no evidence of leaning or broadening. The aspect ratio (H/W) achieved in this case was ~3.5.

Contact angle

For comparison with the literature value, the contact angle of water on native PDMS as measured on our setup was 102°, which is consistent with that reported by Hillborg *et al.*[45] The UV-cured PUMA substrate had a contact angle of 72°, which is significantly more hydrophilic compared to PDMS. This value is close to the reported value of polyurethane,[46] which is a major component of this resin. Treatment with oxygen plasma for 6 min reduced the contact angle of PUMA to 53°, which is also in agreement with the behavior of oxidized polyurethane.[46] Plasma reduction of contact angle was reversed by baking at 75 °C in a sealed glass jar for 2 days; the contact angle returned to 75°, which is within statistical agreement with the native PUMA substrate.

Optical properties

Cured PUMA is optically clear, with a refractive index of 1.504. Fig. 4A plots the optical transmission through PUMA over 200–1000 nm, along with that of TPE, PDMS, and glass. PUMA has a similar optical clarity as glass in the visible range; however, because of the presence of UV photoinitiator for crosslinking, one naturally expects a sharp absorption in the UV range. Thus PUMA, like TPE, is not particularly suitable for UV absorbance applications.

Fig. 4B shows the autofluorescence by the polymer substrates under 488 and 633 nm excitation. The autofluorescence level of all three polymer substrates decayed over time, consistent with observations in other plastic materials.[47] Fig. 4B inset compares the maximum autofluorescence level of PDMS, PUMA, and TPE: PUMA exhibited less autofluorescence than TPE but more than PDMS. This level of autofluorescence is suitable for most applications involving fluorescence detection. For high-sensitivity single-molecule work, however, a confocal detection geometry that can reject efficiently background signal from the substrate should be employed.

Chemical compatibility

Table 2 tabulates the observed swelling ratio of PUMA discs in each chemical after 24 h immersion. PUMA was found to be very

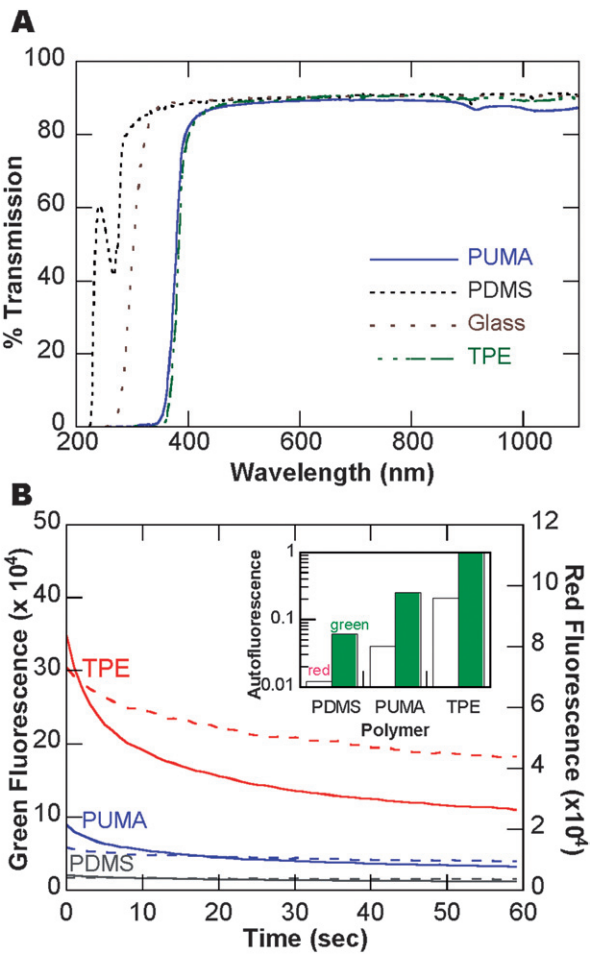

Fig. 4 (**A**) Optical transmission characteristics of PUMA, PDMS, Glass, and TPE. (**B**) Green fluorescence (solid lines; 510–565 nm, $\lambda_{excitation}$ = 488 nm) and red fluorescence (dashed lines; 660–711 nm, $\lambda_{excitation}$ = 633 nm) intensities of TPE, PUMA, and PDMS. **Inset**: Maximum (initial) autofluorescence of each polymer, normalized with respect to the maximum green fluorescence of TPE.

Table 2 Area ratio of PUMA discs after submerging in various solvents for 24 hours

Chemical	Area Ratio PUMA
Acetic acid, 1M	1.0
Hydrochloric acid, 1M	1.0
Ammonium Hydroxide, 1M	1.0
Sodium Hydroxide, 1M	1.0
Acetone	1.3
Acetonitrile	1.1
DMSO	1.5
Formaldehyde	1.0
Heptane	1.1
Tetrahydrofuran	1.8
Methanol	1.4
Ethanol	1.4
2-Propanol	1.2
Fluorescein	1.0
Rhodamine B	1.0
Fluorinert	1.0
Mineral oil	1.0
Perfluorodecalin	1.0
Silicone oil	1.0
Water	1.0

resistant to dyes, acids, bases, water, formaldehyde, mineral oil, silicone oil, Fluorinert, and perfluorodecaline. While most organic solvents at 100% purity caused swelling, PUMA had lower swelling ratios with acetone and acetonitrile than those of TPE.[26] We note that for low molecular weight alcohols such as methanol and ethanol, PUMA appears to have swollen more comparing to polyurethane alone, which had a swelling ratio of ~1.1.[46] For solvents that are commonly used to dissolve dyes or surfactants, we found that at the typical concentrations of usage these solvents had no effect on microfabricated structures. For example, at low concentrations (<5% aqueous solution), neither methanol nor ethanol caused any swelling of features in routine microfluidic experiments. Surfactant solutions (*e.g.* Pluronic F-127) made with DMSO prior to dilution with aqueous phase were also compatible with PUMA microchannels at the typical concentration of usage (~0.1%).

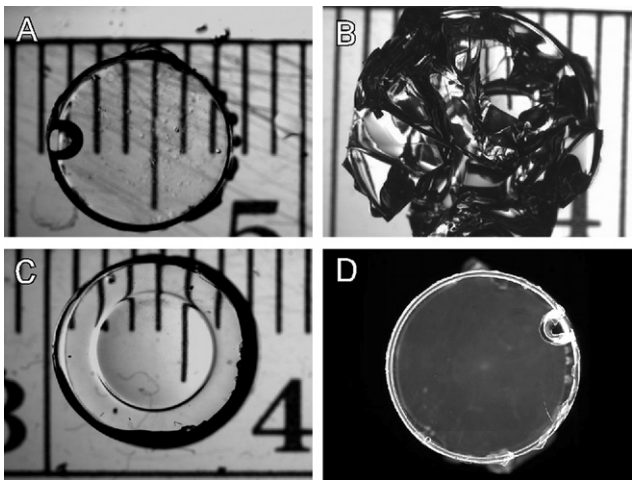

Fig. 5 PUMA discs (6 mm (D) before immersion) submerged for 24 h in (**A**) perfluorodecaline, (**B**) tetrahydrofuran, (**C**) isopropanol, and (**D**) 25 μM Rhodamine B (fluorescence image under 533 nm excitation).

Fig. 5 shows select images of PUMA discs after immersion for 24 h in various organic compounds and dyes to illustrate the effects of immersion. Oils immiscible with water had no effect on the PUMA discs (Fig. 5A). We also conducted additional testing of PUMA by heating samples in mineral oil, Fluorinert, and perfluorodecaline up to 90 °C; no change in circular area or dissolution was observed. This fact should make PUMA compatible with emerging applications in droplet microfluidics, which employ many of these oils. On the other hand, significant swelling was observed in the alcohols, heptane, DMSO, and in particular, tetrahydrofuran, in which severe cracking was observed (Fig. 5B). For some solvents, rather than causing a uniform expansion, some discs formed a depression in the

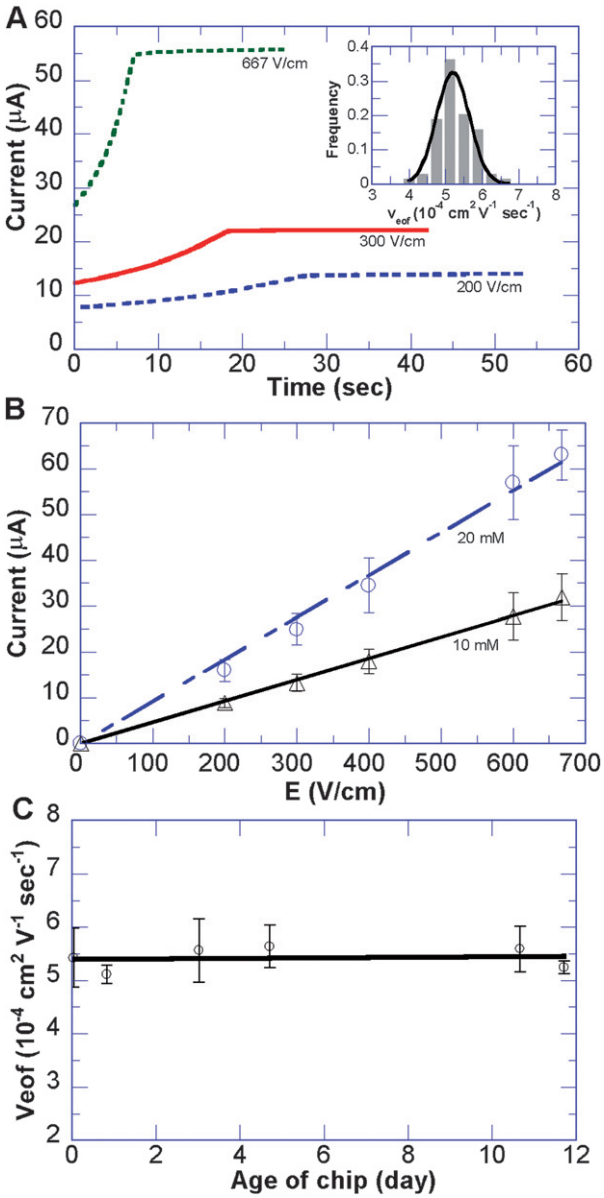

Fig. 6 Electrokinetic characteristics of PUMA substrate. (**A**) Current traces under electrokinetic-driven flow. **Inset**: Statistical distribution of ν_{eof} measurements; $N = 68$. (**B**) Current trace as a function of applied electric field. (**C**) ν_{eof} as a function of the age of PUMA chips after bonding.

center as a result of immersion (Fig. 5C, with isopropanol). This is likely due to a slower rate of penetration such that after 24 h the center of the disc remained largely unaffected.

Dye penetration was observed in PUMA discs immersed in 25 μM Rhodamine B (Fig. 5D) but was not observed in fluorescein. Dye penetration by Rhodamine B is disappointing but not unexpected as Rhodamine B is known to penetrate most polymeric materials.

Electroosmotic flow

Native PUMA exhibited very strong electroosmotic mobility; the EOF moves toward cathode, the same direction as in PDMS, glass, and TPE. This would suggest that the native PUMA surface also exhibited negative charge under the buffer environment used. In borate buffer, v_{eof}, the electroosmotic mobility of PUMA, was 5.5×10^{-4} cm^2 $V^{-1}sec^{-1}$, quite comparable to that of fused-silica capillary; Fig. 6A inset shows the statistical distribution of electroosmotic mobility measurements. This value is ~2 times higher than that of thermal-cured polyurethane reported in the literature.[46] Fig. 6A shows how the electrical current stabilized when the anode reservoir was replaced with 20 mM borate buffer. As the EOF drove the 20 mM buffer solution in anode reservoir to displace the 10 mM buffer previously in the channel, the ionic strength increased and led to an increase of electrical current until the entire channel was filled with 20 mM buffer. As the electric field increased from 200 V cm^{-1} to 667 V cm^{-1} (the maximum output from our power supply), the time to reach a new steady state decreased as expected. Within the range of electric field that we applied, we did not notice any Joule heating. Fig. 6B plots the electrical current measured using 10 and 20 mM borate buffers as a function of the applied electric field. Up to 667 V cm^{-1}, these relationships were linear, indicating no alteration in ionic conductivity from Joule heating.

Unlike PDMS or TPE, PUMA surface did not need to be oxidized to achieve high EOF; in addition, the electroosmotic mobility was remarkably stable after manufacturing. Fig. 6C shows the electroosmotic mobility as measured on different days following manufacturing; to avoid systemic sampling errors associated with sampling from only a single production run, different chips of various ages selected from three production runs were used for each measurement. As shown in Fig. 6C, the mean (horizontal line) was invariant with respect to chip age up to 12 days.

Conclusion

PUMA is a promising material for fabricating microfluidic devices for disposable use in clinical situations. Because the raw material has already been qualified as USP Class VI-compliant, its working temperature, biocompatibility, and sterilizability have been well characterized and devices fabricated from this material can be expected to meet regulatory approval. This paper reported a production process that offered high-fidelity microstructure replication in particular at high density and high-aspect ratio. Similar to hot-embossing and injection-molding, UV-casting offers high production throughput and therefore a viable economic model for disposable devices; however, UV-casting does not require a specialized heated press or molding equipment. This UV-casting production process can be based on either existing PDMS molds fabricated from SU-8-on-Si master or from DRIE-etched Si masters. In addition, as PUMA is a thermoplastic, bonding to form an enclosed microfluidic device is simple: in this instance we simply left the conformally-sealed chips under UV source for 10 min. The resulting seal routinely withstood sustained flow up to 40 psi in our laboratory applications. With these characteristics, we anticipate PUMA to be a useful substrate in the fabrication of disposable microfluidic biomedical devices.

Acknowledgements

We are grateful to Washington State's Life Sciences Discovery Fund (LSDF), the National Institutes of Health (EB005197), and the Keck Foundation for the support of this work.

References

1 P. A. Auroux, D. Iossifidis, D. R. Reyes and A. Manz, *Anal. Chem.*, 2002, **74**, 2637–2652.
2 D. R. Reyes, D. Iossifidis, P. A. Auroux and A. Manz, *Anal. Chem.*, 2002, **74**, 2623–2636.
3 C. S. Effenhauser, A. Manz and H. M. Widmer, *Anal. Chem.*, 1993, **65**, 2637–2642.
4 C. T. Culbertson, S. C. Jacobson and J. M. Ramsey, *Anal. Chem.*, 1998, **70**, 3781–3789.
5 S. C. Jacobson, R. Hergenroder, L. B. Koutny and J. M. Ramsey, *Anal. Chem.*, 1994, **66**, 2369–2373.
6 D. J. Harrison, A. Manz, Z. H. Fan, H. Ludi and H. M. Widmer, *Anal. Chem.*, 1992, **64**, 1926–1932.
7 S. C. Terry, J. H. Jerman and J. B. Angell, *IEEE Trans. Electron Devices*, 1979, **26**, 1880–1886.
8 A. T. Woolley and R. A. Mathies, *Proc. Natl. Acad. Sci. U. S. A.*, 1994, **91**, 11348–11352.
9 C. S. Effenhauser, G. J. M. Bruin, A. Paulus and M. Ehrat, *Anal. Chem.*, 1997, **69**, 3451–3457.
10 G. S. Fiorini and D. T. Chiu, *Biotechniques*, 2005, **38**, 429–446.
11 H. Becker and U. Heim, *Sens. Actuators, A*, 2000, **83**, 130–135.
12 A. C. Henry, T. J. Tutt, M. Galloway, Y. Y. Davidson, C. S. McWhorter, S. A. Soper and R. L. McCarley, *Anal. Chem.*, 2000, **72**, 5331–5337.
13 N. L. Jeon, D. T. Chiu, C. J. Wargo, H. K. Wu, I. S. Choi, J. R. Anderson and G. M. Whitesides, *Biomed. Microdevices*, 2002, **4**, 117–121.
14 B. H. Jo, L. M. Van Lerberghe, K. M. Motsegood and D. J. Beebe, *J. Microelectromech. Syst.*, 2000, **9**, 76–81.
15 J. Kameoka, H. G. Craighead, H. W. Zhang and J. Henion, *Anal. Chem.*, 2001, **73**, 1935–1941.
16 L. Martynova, L. E. Locascio, M. Gaitan, G. W. Kramer, R. G. Christensen and W. A. MacCrehan, *Anal. Chem.*, 1997, **69**, 4783–4789.
17 R. M. McCormick, R. J. Nelson, M. G. AlonsoAmigo, J. Benvegnu and H. H. Hooper, *Anal. Chem.*, 1997, **69**, 2626–2630.
18 S. Z. Qi, X. Z. Liu, S. Ford, J. Barrows, G. Thomas, K. Kelly, A. McCandless, K. Lian, J. Goettert and S. A. Soper, *Lab Chip*, 2002, **2**, 88–95.
19 M. A. Unger, H. P. Chou, T. Thorsen, A. Scherer and S. R. Quake, *Science*, 2000, **288**, 113–116.
20 J. D. Xu, L. Locascio, M. Gaitan and C. S. Lee, *Anal. Chem.*, 2000, **72**, 1930–1933.
21 G. M. Whitesides, E. Ostuni, S. Takayama, X. Y. Jiang and D. E. Ingber, *Annu. Rev. Biomed. Eng.*, 2001, **3**, 335–373.
22 J. R. Anderson, D. T. Chiu, R. J. Jackman, O. Cherniavskaya, J. C. McDonald, H. K. Wu, S. H. Whitesides and G. M. Whitesides, *Anal. Chem.*, 2000, **72**, 3158–3164.
23 D. C. Duffy, J. C. McDonald, O. J. A. Schueller and G. M. Whitesides, *Anal. Chem.*, 1998, **70**, 4974–4984.

24 J. C. McDonald, D. C. Duffy, J. R. Anderson, D. T. Chiu, H. K. Wu, O. J. A. Schueller and G. M. Whitesides, *Electrophoresis*, 2000, **21**, 27–40.
25 J. C. McDonald and G. M. Whitesides, *Acc. Chem. Res.*, 2002, **35**, 491–499.
26 G. S. Fiorini, R. M. Lorenz, J. S. Kuo and D. T. Chiu, *Anal. Chem.*, 2004, **76**, 4697–4704.
27 H. Makamba, J. H. Kim, K. Lim, N. Park and J. H. Hahn, *Electrophoresis*, 2003, **24**, 3607–3619.
28 S. W. Hu, X. Q. Ren, M. Bachman, C. E. Sims, G. P. Li and N. L. Allbritton, *Anal. Chem.*, 2004, **76**, 1865–1870.
29 S. W. Hu, X. Q. Ren, M. Bachman, C. E. Sims, G. P. Li and N. L. Allbritton, *Langmuir*, 2004, **20**, 5569–5574.
30 S. J. Choi, K. Y. Suh and H. H. Lee, *J. Am. Chem. Soc.*, 2008, **130**, 6312.
31 Z. T. Cygan, J. T. Cabral, K. L. Beers and E. J. Amis, *Langmuir*, 2005, **21**, 3629–3634.
32 L. H. Hung, R. Lin and A. P. Lee, *Lab Chip*, 2008, **8**, 983–987.
33 P. J. A. Kenis and A. D. Stroock, *MRS Bull.*, 2006, **31**, 87–94.
34 P. Kim, H. E. Jeong, A. Khademhosseini and K. Y. Suh, *Lab Chip*, 2006, **6**, 1432–1437.
35 J. K. Liu, X. F. Sun and M. L. Lee, *Anal. Chem.*, 2007, **79**, 1926–1931.
36 J. P. Rolland, R. M. Van Dam, D. A. Schorzman, S. R. Quake and J. M. DeSimone, *J. Am. Chem. Soc.*, 2004, **126**, 2322–2323.
37 T. T. Truong, R. S. Lin, S. Jeon, H. H. Lee, J. Maria, A. Gaur, F. Hua, I. Meinel and J. A. Rogers, *Langmuir*, 2007, **23**, 2898–2905.
38 G. S. Fiorini, M. Yim, G. D. M. Jeffries, P. G. Schiro, S. A. Mutch, R. M. Lorenz and D. T. Chiu, *Lab Chip*, 2007, **7**, 923–926.
39 S. H. Kim, Y. Yang, M. Kim, S. W. Nam, K. M. Lee, N. Y. Lee, Y. S. Kim and S. Park, *Adv. Funct. Mater.*, 2007, **17**, 3493–3498.
40 W. X. Zhou and M. B. Chan-Park, *Lab Chip*, 2005, **5**, 512–518.
41 *United States Pharmacopeia 23 - National Formulary 18*, United States Pharmacopeial Convention, Rockville, Maryland, 1994, ch. 87–88.
42 X. H. Huang, M. J. Gordon and R. N. Zare, *Anal. Chem.*, 1988, **60**, 1837–1838.
43 L. E. Locascio, C. E. Perso and C. S. Lee, *J. Chromatogr., A*, 1999, **857**, 275–284.
44 N. Bowden, S. Brittain, A. G. Evans, J. W. Hutchinson and G. M. Whitesides, *Nature*, 1998, **393**, 146–149.
45 H. Hillborg, J. F. Ankner, U. W. Gedde, G. D. Smith, H. K. Yasuda and K. Wikstrom, *Polymer*, 2000, **41**, 6851–6863.
46 E. Piccin, W. K. T. Coltro, J. A. F. da Silva, S. C. Neto, L. H. Mazo and E. Carrilho, *J. Chromatogr., A*, 2007, **1173**, 151–158.
47 A. Piruska, I. Nikcevic, S. H. Lee, C. Ahn, W. R. Heineman, P. A. Limbach and C. J. Seliskar, *Lab Chip*, 2005, **5**, 1348–1354.

